

UNITED STATES AIR FORCE  
RESEARCH LABORATORY

---

NUMERICAL STUDY OF SHORT OPTICAL  
PULSE PROPAGATION IN NONLINEAR  
REVERSE SATURABLE ABSORBERS

Sukkeun Kim

Courant Institute of Mathematical Sciences  
New York University  
New York, NY

Mary Potasek

HUMAN EFFECTIVENESS DIRECTORATE  
DIRECTED ENERGY BIOEFFECTS DIVISION  
BIOMECHANISMS AND MODELING BRANCH  
2509 Gillingham Drive  
Brooks AFB, TX 78235-5215

February 2001

Approved for public release; distribution is unlimited.

20010323 080

## NOTICES

**This report is published in the interest of scientific and technical information exchange and does not constitute approval or disapproval of its ideas or findings.**

**Using Government drawings, specifications, or other data included in this document for any purpose other than Government-related procurement does not in any way obligate the US Government. The fact that the Government formulated or supplied the drawings, specifications, or other data, does not license the holder or any other person or corporation, or convey any rights or permission to manufacture, use, or sell any patented invention that may relate to them.**

**The Office of Public Affairs has reviewed this report, and it is releasable to the National Technical Information Service, where it will be available to the general public, including foreign nationals.**

**This report has been reviewed and is approved for publication.**



**MARY J. POTASEK, Ph.D.  
Project Scientist**



**RICHARD L. MILLER, Ph.D.  
Chief, Directed Energy Bioeffects Division**

## REPORT DOCUMENTATION PAGE

Form Approved  
OMB No. 0704-01-0188

The public reporting burden for this collection of information is estimated to average 1 hour per response, including the time for reviewing instructions, searching existing data sources, gathering and maintaining the data needed, and completing and reviewing the collection of information. Send comments regarding this burden estimate or any other aspect of this collection of information, including suggestions for reducing the burden to Department of Defense, Washington Headquarters Services Directorate for Information Operations and Reports (0704-0188), 1215 Jefferson Davis Highway, Suite 1204, Arlington VA 22202-4302. Respondents should be aware that notwithstanding any other provision of law, no person shall be subject to any penalty for failing to comply with a collection of information if it does not display a currently valid OMB control number.

PLEASE DO NOT RETURN YOUR FORM TO THE ABOVE ADDRESS.

1. REPORT DATE (DD-MM-YYYY) 12-02-2001	2. REPORT TYPE Interim Report	3. DATES COVERED (From - To) Jan 2000 - Dec 2000		
4. TITLE AND SUBTITLE Numerical Study of Short Optical Pulse Propagation in Nonlinear Reverse Saturable Absorbers		5a. CONTRACT NUMBER		
		5b. GRANT NUMBER		
		5c. PROGRAM ELEMENT NUMBER 62202F		
6. AUTHORS Sukkeun Kim Mary Potasek		5d. PROJECT NUMBER 7757, 2304		
		5e. TASK NUMBER B4, W1		
		5f. WORK UNIT NUMBER 05, 01		
7. PERFORMING ORGANIZATION NAME(S) AND ADDRESS(ES) Courant Institute of Mathematical Sciences New York University New York, NY		8. PERFORMING ORGANIZATION REPORT NUMBER		
9. SPONSORING/MONITORING AGENCY NAME(S) AND ADDRESS(ES) Air Force Research Laboratory Human Effectiveness Directorate Directed Energy Bioeffects Division Biomechanisms and Modeling Branch 2509 Gillingham Drive, Brooks AFB, TX 78235-5118		10. SPONSOR/MONITOR'S ACRONYM(S) AFRL, HE		
		11. SPONSOR/MONITOR'S REPORT NUMBER(S) AFRL-HE-BR-TR-2001-0009		
12. DISTRIBUTION/AVAILABILITY STATEMENT Approved for public release; distribution unlimited.				
13. SUPPLEMENTARY NOTES				
14. ABSTRACT We derived a numerical method for the propagation of the electromagnetic pulse in nonlinear reverse saturable absorbers. This method includes the nonlinear Kerr effect, dispersion, diffraction and reverse saturable absorption which is expressed in terms of a five-level model. This report describes derivation of the nonlinear wave equation, the reverse saturable absorption rate equations, and the numerical method.				
15. SUBJECT TERMS Laser, Nonlinear optics, Pulse propagation, Electromagnetics, Optical Limiting, Reverse Saturable Absorber				
16. SECURITY CLASSIFICATION OF: a. REPORT U b. ABSTRACT U c. THIS PAGE U		17. LIMITATION OF ABSTRACT UU	18. NUMBER OF PAGES 26	19a. NAME OF RESPONSIBLE PERSON Dr. Mary Potasek
				19b. TELEPHONE NUMBER (Include area code) (210) 536- 5709

## **Contents**

<b>1</b>	<b>INTRODUCTION</b>	<b>1</b>
<b>2</b>	<b>NONLINEAR WAVE EQUATION</b>	<b>2</b>
<b>3</b>	<b>NONLINEAR POLARIZATION</b>	<b>5</b>
<b>4</b>	<b>SCALED NONLINEAR WAVE EQUATION</b>	<b>6</b>
<b>5</b>	<b>RSA RATE EQUATION</b>	<b>7</b>
<b>6</b>	<b>SPLIT-STEP METHOD</b>	<b>9</b>
<b>7</b>	<b>NUMERICAL CALCULATION</b>	<b>10</b>
7.1	Diffraction Operator . . . . .	10
7.2	Dispersion Operator . . . . .	13
7.3	Nonlinear Operator . . . . .	13
7.4	Rate Equation . . . . .	14
<b>8</b>	<b>ITERATION</b>	<b>15</b>
<b>9</b>	<b>SOLITON SOLUTION</b>	<b>16</b>
<b>10</b>	<b>CONCLUSION</b>	<b>16</b>
<b>ACKNOWLEDGEMENTS</b>		<b>16</b>
<b>BIBLIOGRAPHY</b>		<b>17</b>

## List of Figures

1	Schematic energy level for a chromophore. The electronic states are represented by solid horizontal lines and the vibronic states are represented by dotted horizontal lines. $S_i$ represents a singlet state and $T_i$ represents a triplet state. The photon absorption excitations are represented by solid vertical lines, and the decay processes are represented by wavy lines. The absorption coefficients $\sigma_{ij}$ and the decay constants $k_{ij}$ are described in the text. The physical values used for our calculations are: $\sigma_{01} = 2.4 \times 10^{-18} cm^2$ , $\sigma_{12} = 3.0 \times 10^{-17} cm^2$ , $\sigma_{34} = 4.8 \times 10^{-17} cm^2$ , $k_{10} = 0.144 ns^{-1}$ , $k_{21} = 1.0 ps^{-1}$ , $k_{13} = 77.8 ms^{-1}$ , $k_{30} = 50.0 ms^{-1}$ , $k_{43} = 1.0 ps^{-1}$ , and $k_{11}$ , $k_{22}$ , $k_{33}$ are due to vibrational decays which are assumed to be instantaneous. . . . .	19
2	Space-Time grid for pulse propagation. Squares represent coordinates where pulse is calculated and circles represent coordinates where carrier densities are calculated. . . . .	20
3	Analytic and numerical solution for the fundamental soliton propagation. The solid line shows the analytic solution and the circles show the numerical solution. . . . .	20
4	Relative error of and numerical solution for the fundamental soliton propagation. . . . .	21

# Numerical study of short optical pulse propagation in nonlinear reverse saturable absorbers

## 1 INTRODUCTION

Recent developments in short pulse laser systems have introduced growing studies in the problem of ultra short pulse propagation in nonlinear media. Competitions among the effects of nonlinearity, diffraction, and group velocity dispersion (GVD) give rich spatiotemporal phenomena such as self-focusing[1], self-defocusing, and pulse splitting. Understanding of short pulse propagation is very important for protection of human eyes and optical equipment from high power laser pulses. Optical limiters are needed that give high transmittance at low input intensities and low transmittance at high input intensities. There are various mechanisms that result from nonlinear optical responses such as nonlinear absorption, nonlinear scattering and nonlinear refraction[2]. Desirable properties for optical limiting candidates include, a high linear transmittance, a potentially low limiting threshold, a rapid response of picoseconds or faster, a broad spectral response, and a large dynamic range. Some semiconductors, gases and liquid crystals are used as optical limiting materials[3, 4]. Liquid crystals exhibit high refractive nonlinearities but low response time (nanoseconds). Chromophores exhibiting nonlinear absorption, such as reverse saturable absorption (RSA), are under consideration for optical limiting applications[5, 6, 7]. In a molecular system, RSA arises when the excited state absorption cross section is larger than the ground state absorption cross section. The process is modeled by several vibronically broadened electronic energy levels. The general situation involves a five level system. The energy states included are three levels of the singlet state coupled to two levels of an excited triplet state. The mechanism of RSA is described in terms of simple rate equations coupled to a one-dimensional propagation equation of the optical pulse intensity. Figure 1 shows the energy level diagram for the five-state model. Other materials and mechanisms have been used such as fullerenes[8, 9], carbon black suspension[10, 11], and two-photon absorption[12, 13]. While the main material studied in this paper is RSA, these materials are usually incorporated in a host material. With the recent introduction of novel high power lasers, the propagation of light in nonlinear materials is often subject to various phenomena such as self-focusing or self-phase modulation[14, 15, 16, 17, 18]. These effects are just beginning to be studied in RSA materials. Therefore, in order to study these effects we derived an equation[19] for the propagation of the electromagnetic field coupled to the rate equations because the traditional equations, which use only the pulse intensity, cannot answer these more detailed questions. Yet this equation cannot be solved analytically, therefore in this report we use numerical

methods. The principle numerical method is the split-step beam propagation method (BPM) that is coupled to a finite difference technique. One significant result is that, under certain circumstances, self-focusing can enhance the power limiting properties of RSA materials.

## 2 NONLINEAR WAVE EQUATION

From Maxwell's equations we obtain the following wave equation

$$\left( \nabla^2 - \frac{1}{c^2} \frac{\partial^2}{\partial t^2} \right) E(\vec{r}, t) - \frac{1}{\epsilon_0 c^2} \frac{\partial^2}{\partial t^2} P(\vec{r}, t) = 0, \quad (1)$$

where we assume that  $\nabla \cdot \vec{E} = 0$  and  $\vec{E} \parallel \vec{P}$ . The electric polarization can be expressed as a sum of two parts such as the linear part  $P_l$  and the nonlinear part  $P_{nl}$

$$P(\vec{r}, t) = P_l(\vec{r}, t) + P_{nl}(\vec{r}, t), \quad (2)$$

and the linear part is related to the electric field by the following relation

$$P_l(\vec{r}, t) = \epsilon \int_{-\infty}^t \chi(t-t') \cdot E(\vec{r}, t') dt'. \quad (3)$$

Then the wave equation in the frequency domain becomes

$$\left[ \nabla^2 + \epsilon(\omega) \frac{\omega^2}{c^2} \right] \tilde{E}(\vec{r}, \omega) + \frac{\omega^2}{\epsilon_0 c^2} \tilde{P}_{nl}(\vec{r}, \omega) = 0, \quad (4)$$

where

$$\epsilon(\omega) = 1 + \chi(\omega), \quad (5)$$

$$\tilde{E}(\vec{r}, \omega) = \int_{-\infty}^{\infty} E(\vec{r}, t) e^{-i\omega t} dt, \quad (6)$$

$$\tilde{P}_{nl}(\vec{r}, \omega) = \int_{-\infty}^{\infty} P_{nl}(\vec{r}, t) e^{-i\omega t} dt. \quad (7)$$

In the slowly varying envelope approximation, it is useful to separate the rapidly varying part of the electric field as

$$E(\vec{r}, t) = A(\vec{r}, t) e^{ik_0 z - i\omega_0 t} + c.c., \quad (8)$$

$$P_{nl}(\vec{r}, t) = B(\vec{r}, t) e^{ik_0 z - i\omega_0 t} + c.c., \quad (9)$$

and  $A$  and  $B$  are slowly varying envelopes which satisfies the following conditions

$$\left| \frac{\partial A}{\partial x_i} \right| \ll k_0 |A|, \quad \left| \frac{\partial B}{\partial x_i} \right| \ll k_0 |B|, \quad (10)$$

$$\left| \frac{\partial A}{\partial t} \right| \ll \omega_0 |A|, \quad \left| \frac{\partial B}{\partial t} \right| \ll \omega_0 |B|, \quad (11)$$

where  $x_i = x, y, z$ . In the frequency domain, the electric field and the nonlinear polarization become

$$\tilde{E}(\vec{r}, \omega) = \tilde{A}(\vec{r}, \omega - \omega_0)e^{+ik_0z} + \tilde{A}^*(\vec{r}, \omega + \omega_0)e^{-ik_0z}, \quad (12)$$

$$\tilde{P}_{nl}(\vec{r}, \omega) = \tilde{B}(\vec{r}, \omega - \omega_0)e^{+ik_0z} + \tilde{B}^*(\vec{r}, \omega + \omega_0)e^{-ik_0z}. \quad (13)$$

Then the wave equation becomes

$$\left[ \nabla_{\perp}^2 + \left( \frac{\partial}{\partial z} + ik_0 \right)^2 + \epsilon(\omega) \frac{\omega^2}{c^2} \right] \tilde{A}(\vec{r}, \omega - \omega_0) + \frac{\omega^2}{\epsilon_0 c^2} \tilde{B}(\vec{r}, \omega - \omega_0) = 0, \quad (14)$$

where  $\nabla_{\perp}^2 = \partial^2/\partial x^2 + \partial^2/\partial y^2$  and we assume that  $e^{i(kz-\omega t)}$  terms and  $e^{-i(kz-\omega t)}$  terms are separable. Defining  $k(\omega) = \sqrt{\epsilon(\omega)}\omega/c$  we get the Taylor series expansion of  $k(\omega)$  and  $\omega^2$  around  $\omega_0$ . By inverse Fourier transformation, we obtain the following wave equation in the time domain

$$\left[ \nabla_{\perp}^2 + \left( \frac{\partial}{\partial z} + ik_0 \right)^2 + \left( \sum_{n=0}^{\infty} \frac{k^{(n)}(\omega_0)}{n!} \left( i \frac{\partial}{\partial t} \right)^n \right)^2 \right] A(\vec{r}, t) + \frac{1}{\epsilon_0 c^2} \left( i \frac{\partial}{\partial t} + \omega_0 \right)^2 B(\vec{r}, t) = 0, \quad (15)$$

where

$$k^{(n)}(\omega_0) = \left. \frac{\partial^n k(\omega)}{\partial \omega^n} \right|_{\omega_0}. \quad (16)$$

Defining the terms

$$k^{(0)}(\omega_0) = k_0 + i \frac{\alpha_0}{2}, \quad (17)$$

$$k^{(1)}(\omega_0) = k_1 + i \frac{\alpha_1}{2}, \quad (18)$$

we obtain the operator

$$\hat{D}(\omega_0) = i \frac{\alpha_0}{2} - \frac{\alpha_1}{2} \partial_t + \sum_{n=2}^{\infty} \frac{k^{(n)}(\omega_0)}{n!}. \quad (19)$$

Using Eq. (17-19), the wave equation can be expressed as

$$\left[ \nabla_{\perp}^2 + \left( \frac{\partial}{\partial z} + 2ik_0 - k_1 \frac{\partial}{\partial t} + i\hat{D} \right) \left( \frac{\partial}{\partial z} + k_1 \frac{\partial}{\partial t} - i\hat{D} \right) \right] A(\vec{r}, t) + \frac{1}{\epsilon_0 c^2} \left( i \frac{\partial}{\partial t} + \omega_0 \right)^2 B(\vec{r}, t) = 0. \quad (20)$$

In the moving reference frame defined by,  $T = t - k_1 z$ ,  $\xi = z$ , the derivatives become

$$\frac{\partial}{\partial z} = \frac{\partial}{\partial \xi} - k_1 \frac{\partial}{\partial T}, \quad \frac{\partial}{\partial t} = \frac{\partial}{\partial T}. \quad (21)$$

Then the wave equation becomes

$$\left[ \nabla_{\perp}^2 + \left( \frac{\partial}{\partial \xi} + 2ik_0 - 2k_1 \frac{\partial}{\partial T} + i\hat{D} \right) \left( \frac{\partial}{\partial \xi} - i\hat{D} \right) \right] A(\vec{r}, T) + \frac{1}{\epsilon_0 c^2} \left( i \frac{\partial}{\partial T} + \omega_0 \right)^2 B(\vec{r}, T) = 0. \quad (22)$$

Reordering the terms

$$2ik_0 - 2k_1 \frac{\partial}{\partial T} = 2ik_0 - \frac{2k_0}{\omega_0} \frac{\partial}{\partial T} + \frac{2k_0}{\omega_0} \frac{\partial}{\partial T} - 2k_1 \frac{\partial}{\partial T} = 2ik_0 \left( 1 + \frac{i}{\omega_0} \frac{\partial}{\partial T} \right) + 2 \left( \frac{k_0}{\omega_0} - k_1 \right) \frac{\partial}{\partial T}, \quad (23)$$

and using Eq (23) in Eq (22), we obtain

$$\begin{aligned} & \left[ \nabla_{\perp}^2 + 2ik_0 \left( 1 + \frac{i}{\omega_0} \frac{\partial}{\partial T} \right) \left( \frac{\partial}{\partial \xi} - i\hat{D} \right) \right] A(\vec{r}, T) + \frac{\omega_0^2}{\epsilon_0 c^2} \left( 1 + \frac{i}{\omega_0} \frac{\partial}{\partial T} \right)^2 B(\vec{r}, T) \\ &= - \left[ \frac{\partial}{\partial \xi} + i\hat{D} + 2 \left( \frac{k_0}{\omega_0} - k_1 \right) \frac{\partial}{\partial T} \right] \left[ \frac{\partial}{\partial \xi} - i\hat{D} \right] A(\vec{r}, t). \end{aligned} \quad (24)$$

From the definition of  $k(\omega)$ , we obtain

$$\frac{\partial k}{\partial \omega} = \frac{\omega}{c} \frac{\partial \sqrt{\epsilon}}{\partial \omega} + \frac{\sqrt{\epsilon}}{c}, \quad (25)$$

$$k_1 = \operatorname{Re} \left( \frac{\partial \sqrt{\epsilon}}{\partial \omega} \Big|_{\omega_0} \right) \frac{\omega_0}{c} + \frac{k_0}{\omega_0}, \quad (26)$$

where

$$k_1 = \frac{k_0}{\omega_0}, \quad \text{if } \frac{\partial \sqrt{\epsilon}}{\partial \omega} \ll \frac{\sqrt{\epsilon}}{\omega}. \quad (27)$$

If the right-hand side of Eq. (24) is very small, then Eq. (24) becomes

$$\frac{\partial A}{\partial \xi} \approx \left[ i\hat{D} + \frac{i}{2k_0} \left( 1 + \frac{i}{\omega_0} \frac{\partial}{\partial T} \right)^{-1} \nabla_{\perp}^2 \right] A + \frac{i}{2k_0} \frac{\omega_0^2}{\epsilon_0 c^2} \left( 1 + \frac{i}{\omega_0} \frac{\partial}{\partial T} \right) B. \quad (28)$$

If we assume

$$\left( 1 + \frac{i}{\omega_0} \frac{\partial}{\partial T} \right)^{-1} \approx 1 - \frac{i}{\omega_0} \frac{\partial}{\partial T}, \quad (29)$$

$$\hat{D} \approx i \frac{\alpha_0}{2} + \frac{k_2}{2} \left( i \frac{\partial}{\partial T} \right)^2 + \frac{k_3}{6} \left( i \frac{\partial}{\partial T} \right)^3, \quad (30)$$

then Eq. (28) becomes

$$\frac{\partial A}{\partial \xi} \approx \left[ \frac{\alpha_0}{2} - i \frac{k_2}{2} \frac{\partial^2}{\partial T^2} + \frac{k_3}{6} \frac{\partial^3}{\partial T^3} + \frac{i}{2k_0} \left( 1 - \frac{i}{\omega_0} \frac{\partial}{\partial T} \right) \nabla_{\perp}^2 \right] A + \frac{i}{2k_0} \frac{\omega_0^2}{\epsilon_0 c^2} \left( 1 + \frac{i}{\omega_0} \frac{\partial}{\partial T} \right) B. \quad (31)$$

### 3 NONLINEAR POLARIZATION

If we consider only the third-order nonlinear effects governed by  $\chi^{(3)}$ , then the nonlinear polarization becomes

$$P_{nl}(\vec{r}, t) = \epsilon_0 \int_{-\infty}^t \int_{-\infty}^t \int_{-\infty}^t \chi^{(3)}(t - t_1, t - t_2, t - t_3) E(\vec{r}, t_1) E(\vec{r}, t_2) E(\vec{r}, t_3) dt_1, dt_2, dt_3. \quad (32)$$

We further assume the following functional form for the third-order susceptibility,

$$\chi^{(3)}(t - t_1, t - t_2, t - t_3) = \chi^{(3)} R(t - t_1) \delta(t - t_2) \delta(t - t_3), \quad (33)$$

where  $\delta(t)$  is the delta function and  $R(t)$  is the nonlinear response function normalized as  $\int_{-\infty}^{\infty} R(t) dt = 1$ . Then the nonlinear polarization is given by

$$P_{nl}(\vec{r}, t) = \epsilon_0 \chi^{(3)} E(\vec{r}, t) \int_{-\infty}^t R(t - t') E^2(\vec{r}, t') dt', \quad (34)$$

here we assumed  $\vec{E} \parallel \vec{P}_{nl}$ . If the response function  $R(t)$  is nearly instantaneous, we can apply the following Taylor series expansion

$$\begin{aligned} \int_{-\infty}^t R(t - t_1) E^2(\vec{r}, t_1) dt_1 &= \int_{-\infty}^t R(t - t_1) \left[ 1 + \sum_{n=1}^{\infty} \frac{(t_1 - t)^n}{n!} \frac{\partial^n}{\partial t^n} \right] dt_1 E^2(\vec{r}, t) \\ &\approx \left( 1 - T_R \frac{\partial}{\partial t} \right) E^2(\vec{r}, t), \end{aligned} \quad (35)$$

where  $T_R = \int_0^{\infty} t R(t) dt$ . Then the nonlinear polarization becomes

$$P_{nl}(\vec{r}, t) \approx \epsilon_0 \chi^{(3)} E(\vec{r}, t) \left( 1 - T_R \frac{\partial}{\partial t} \right) E^2(\vec{r}, t). \quad (36)$$

From the slowly varying envelope approximation, we obtain the following equations

$$E^2 = A^2 e^{2i(k_0 z - \omega_0 t)} + 2|A|^2 + (A^*)^2 e^{-2i(k_0 z - \omega_0 t)}, \quad (37)$$

$$\frac{\partial E^2}{\partial t} = e^{2i(k_0 z - \omega_0 t)} \left( \frac{\partial}{\partial t} - 2i\omega_0 \right) A^2 + 2 \frac{\partial}{\partial t} |A|^2 + e^{-2i(k_0 z - \omega_0 t)} \left( \frac{\partial}{\partial t} + 2i\omega_0 \right) (A^*)^2, \quad (38)$$

$$\begin{aligned} E \left( 1 - T_R \frac{\partial}{\partial t} \right) E^2 &= e^{3i(k_0 z - \omega_0 t)} A \left\{ 1 - \left( \frac{\partial}{\partial t} - 2i\omega_0 \right) \right\} A^2 \\ &\quad + e^{i(k_0 z - \omega_0 t)} \left[ A^* \left\{ 1 - T_R \left( \frac{\partial}{\partial t} - 2i\omega_0 \right) \right\} A^2 + 2A \left( 1 - T_R \frac{\partial}{\partial t} \right) |A|^2 \right] \\ &\quad + e^{-i(k_0 z - \omega_0 t)} \left[ A \left\{ 1 - T_R \left( \frac{\partial}{\partial t} + 2i\omega_0 \right) \right\} (A^*)^2 + 2A^* \left( 1 - T_R \frac{\partial}{\partial t} \right) |A|^2 \right] \\ &\quad + e^{-3i(k_0 z - \omega_0 t)} A^* \left\{ 1 - \left( \frac{\partial}{\partial t} + 2i\omega_0 \right) \right\} (A^*)^2. \end{aligned} \quad (39)$$

Assume that each  $e^{in(k_0 z - \omega_0 t)}$  ( $n = 3, 1, -1, -3$ ) term can be separated from each other, then

$$B \approx \epsilon_0 \chi^{(3)} A \left[ (3 + 2i\omega_0 T_R) |A|^2 - 4T_R A^* \frac{\partial A}{\partial t} - 2T_R A \frac{\partial A^*}{\partial t} \right]. \quad (40)$$

If  $T_R = 0$ , then  $B = 3\epsilon_0 \chi^{(3)} |A|^2 A$  considering to the Kerr nonlinearity. Using Eq. (40) in Eq. (20) we can obtain wave equation which expressed in terms of  $A(\vec{r}, T)$  only.

## 4 SCALED NONLINEAR WAVE EQUATION

For cylindrically symmetric system, we define the following dimensionless parameters

$$\eta = \frac{\xi}{L_{df}}, \quad \rho = \frac{r_\perp}{r_0}, \quad \tau = \frac{T}{T_0}, \quad Q = \frac{A}{A_0}, \quad (41)$$

where  $L_{df}$ ,  $r_0$ ,  $T_0$ ,  $A_0$  are given by the input pulse and  $r_\perp = \sqrt{x^2 + y^2}$ . Using Eq. (41) the wave equation Eq. (31) can be rewritten as

$$L_{df}^{-1} \frac{\partial Q}{\partial \eta} \approx \left\{ \frac{\alpha_0}{2} - i \frac{k_0}{2T_0^2} \frac{\partial^2}{\partial \tau^2} + \frac{k_3}{6T_0^3} \frac{\partial^3}{\partial \tau^3} + \frac{i}{2k_0} \left( 1 - \frac{i}{\omega_0 T_0} \frac{\partial}{\partial \tau} \right) \frac{1}{r_0^2} \nabla_\rho^2 \right\} Q + \frac{i}{2k_0} \frac{\omega_0^2 \chi^{(3)} |A_0|^2}{c^2} B', \quad (42)$$

and  $B'$  is given as

$$\begin{aligned} B' &\approx \left( 1 + \frac{i}{\omega_0 T_0} \frac{\partial}{\partial \tau} \right) Q \left\{ (3 + 2i\omega_0 T_R) |Q|^2 - 4 \frac{T_R}{T_0} Q^* \frac{\partial Q}{\partial \tau} - 2 \frac{T_R}{T_0} Q \frac{\partial Q^*}{\partial \tau} \right\} \\ &\approx 3Q \left[ \left( 1 + \frac{2}{3}i\omega_0 T_R \right) |Q|^2 + \left( \frac{i}{\omega_0 T_0} - \frac{T_R}{T_0} \right) \left\{ 2Q^* \frac{\partial Q}{\partial \tau} + Q \frac{\partial Q^*}{\partial \tau} \right\} \right], \end{aligned} \quad (43)$$

where  $\partial^2/\partial \tau^2$  and higher order terms are neglected. Now we set  $L_{df} = k_0 r_0^2 / 2$  and introduce the following parameters

$$\Gamma = \alpha_0 L_{df}, \quad \gamma = \frac{k_2}{T_0^2} L_{df}, \quad \delta = \frac{k_3}{T_0^3} L_{df}, \quad \sigma = \frac{1}{\omega_0 T_0}, \quad \tau_R = \frac{T_R}{T_0}, \quad p = \frac{3}{2} \frac{\omega_0^2 \chi^{(3)} |A_0|^2}{k_0 c^2} L_{df}. \quad (44)$$

Then Eq. (42) becomes

$$\begin{aligned} \frac{\partial Q}{\partial \eta} &\approx \left\{ -\frac{\Gamma}{2} - \frac{i\gamma}{2} \frac{\partial^2}{\partial \tau^2} + \frac{\delta}{6} \frac{\partial^3}{\partial \tau^3} + \frac{i}{4} \left( 1 - i\sigma \frac{\partial}{\partial \tau} \right) \nabla_\rho^2 \right\} Q \\ &\quad + ip \left\{ \left( 1 + \frac{2\tau_R}{3\sigma} \right) |Q|^2 + (i\sigma - \tau_R) \left( 2Q^* \frac{\partial Q}{\partial \tau} + Q \frac{\partial Q^*}{\partial \tau} \right) \right\} Q. \end{aligned} \quad (45)$$

Next we define two linear operators  $\hat{D}_{ds}(\tau)$  and  $\hat{D}_{df}(\tau)$  and one nonlinear operator  $\hat{N}(\tau)$  such as

$$\hat{D}_{ds}(\tau) = -\frac{i\gamma}{2}\frac{\partial^2}{\partial\tau^2} + \frac{\delta}{6}\frac{\partial^3}{\partial\tau^3} - \frac{\Gamma}{2}, \quad (46)$$

$$\hat{D}_{df}(\tau) = \frac{i}{4}\left(1 - i\sigma\frac{\partial}{\partial\tau}\right)\nabla_\rho^2, \quad (47)$$

$$\hat{N}(\tau) \approx ip|Q|^2. \quad (48)$$

In the frequency domain, the linear operators become

$$\hat{D}_{ds}(\omega) = \frac{i\gamma}{2}\omega^2 + \frac{i\delta}{6}\omega^3 - \frac{\Gamma}{2}, \quad (49)$$

$$\hat{D}_{df}(\omega) = \frac{i}{4}(1 - \sigma\omega)\nabla_\rho^2, \quad (50)$$

here we use  $\hat{F}\left(\frac{\partial^n}{\partial\tau^n}\right) = (-i\omega)^n$  and  $\omega$  is a dimensionless angular frequency which corresponding the dimensionless time  $\tau$ .

## 5 RSA RATE EQUATION

Rate equations for a five-level RSA are

$$\frac{\partial N_0}{\partial t} = -\frac{\sigma_{01}I}{\hbar\omega_0}N_0 + k_{10}N_1 + k_{30}N_3, \quad (51)$$

$$\frac{\partial N_1}{\partial t} = \frac{\sigma_{01}I}{\hbar\omega_0}N_0 - \left(\frac{\sigma_{12}I}{\hbar\omega_0} + k_{10} + k_{13}\right)N_1 + k_{21}N_2, \quad (52)$$

$$\frac{\partial N_2}{\partial t} = \frac{\sigma_{12}I}{\hbar\omega_0}N_1 - k_{21}N_2, \quad (53)$$

$$\frac{\partial N_3}{\partial t} = -\left(\frac{\sigma_{34}I}{\hbar\omega_0} + k_{30}\right)N_3 + k_{13}N_1 + k_{43}N_4, \quad (54)$$

$$\frac{\partial N_4}{\partial t} = \frac{\sigma_{34}I}{\hbar\omega_0}N_3 - k_{43}N_4, \quad (55)$$

where  $N_j$  is the electron number density of the state  $j$ ,  $\sigma_{jk}$  is the absorption cross-section for electron pumping from the state  $j$  to the state  $k$  and  $k_{jk}$  is the decay rate from the state  $j$  to the state  $k$ . The assignment of the electron densities,  $N_j$ , in Fig. 1 is as follows:  $N_0$  corresponds to the ground level of the singlet state,  $S_0$ ;  $N_1$  corresponds to the first excited level of the singlet state,  $S_1$ ;  $N_2$  corresponds to the second excited level of the singlet state,  $S_2$ ;  $N_3$  corresponds to the first excited level of the triplet state,  $T_1$ ; and  $N_4$  corresponds to the second excited level of the triplet state,  $T_2$ . In these materials, the total number,  $N_T$ ,

of electrons is conserved such that  $N_0 + N_1 + N_2 + N_3 + N_4 = N_T$ . The initial population at  $z = 0$  (i.e. before the pulse is incident on the RSA material) is given by  $N_0 = N_T$  and  $N_1 = N_2 = N_3 = N_4 = 0$ . The optical pulse has an input energy flux density  $I$  with angular frequency  $\omega_0$ ,  $\hbar$  is Planck's constant and  $I/\hbar\omega_0$  is the input photon flux.

The propagation equation of the energy flux density in the moving frame becomes

$$\frac{\partial I}{\partial \xi} = -(\sigma_{01}N_0 + \sigma_{12}N_1 + \sigma_{34}N_4)I. \quad (56)$$

If we assume  $I = \alpha\hbar\omega_0|A|^2$  and  $\alpha$  is a constant, then

$$\frac{\partial A}{\partial \xi} = -\frac{1}{2}(\sigma_{01}N_0 + \sigma_{12}N_1 + \sigma_{34}N_4)A. \quad (57)$$

We can rewrite the rate equations and the propagation equation such as

$$\frac{\partial \vec{N}}{\partial t} = \hat{M}\vec{N} = \left[ \hat{G} + \frac{I}{\hbar\omega_0}\hat{H} \right] \vec{N} = \left[ \hat{G} + \alpha|A|^2\hat{H} \right] \vec{N}, \quad (58)$$

$$\frac{\partial A}{\partial \xi} = -\frac{1}{2}(\vec{\sigma} \cdot \vec{N})A, \quad (59)$$

where

$$\vec{N} = \begin{pmatrix} N_0 \\ N_1 \\ N_2 \\ N_3 \\ N_4 \end{pmatrix}, \hat{G} = \begin{pmatrix} 0 & k_{01} & 0 & k_{30} & 0 \\ 0 & -(k_{10}+k_{13}) & k_{21} & 0 & 0 \\ 0 & 0 & -k_{21} & 0 & 0 \\ 0 & k_{13} & 0 & -k_{30} & k_{43} \\ 0 & 0 & 0 & 0 & -k_{43} \end{pmatrix}, \hat{H} = \begin{pmatrix} -\sigma_{01} & 0 & 0 & 0 & 0 \\ \sigma_{01} & -\sigma_{12} & 0 & 0 & 0 \\ 0 & \sigma_{12} & 0 & 0 & 0 \\ 0 & 0 & 0 & -\sigma_{34} & 0 \\ 0 & 0 & 0 & \sigma_{34} & 0 \end{pmatrix}, \quad (60)$$

and

$$\vec{\sigma} \cdot \vec{N} = \sigma_{01}N_0 + \sigma_{12}N_1 + \sigma_{34}N_3. \quad (61)$$

Let's introduce a following dimensionless parameter

$$\vec{\aleph}_i = \frac{N_i}{N_T}. \quad (62)$$

Using dimensionless parameters defined in Eq. (41) and Eq. (62) the rate equations and the propagation equation become

$$\frac{\partial \vec{\aleph}}{\partial \tau} = T_0 \left[ \hat{G} + \alpha|A_0|^2|Q|^2\hat{H} \right] \vec{\aleph}, \quad (63)$$

$$\frac{\partial Q}{\partial \eta} = -\frac{L_{df}N_T}{2}(\vec{\sigma} \cdot \vec{\aleph}) Q. \quad (64)$$

Eq. (57) describes the propagation of a plane wave. However, for a three-dimensional pulse propagation in RSA material imbedded in a nonlinear medium, the pulse propagation equation becomes

$$\frac{\partial Q}{\partial \eta} = [\hat{D}_{ds} + \hat{D}_{df} + \hat{N} + \hat{N}_{rsa}] Q, \quad (65)$$

where  $\hat{N}_{rsa} = -\vec{\sigma} \cdot \vec{N} L_{df} N_T / 2$  and the pulse propagation equation is coupled to the following rate equations

$$\frac{\partial \vec{N}}{\partial \tau} = T_0 [\hat{G} + \alpha |A_0|^2 |Q|^2 \hat{H}] \vec{N}. \quad (66)$$

## 6 SPLIT-STEP METHOD

The nonlinear equation Eq. (65) can be expressed as

$$\frac{\partial Q}{\partial \eta} = [\hat{D}_{ds} + \hat{D}_{df} + \hat{N}_{nl}] Q, \quad (67)$$

where  $\hat{N}_{nl} = \hat{N} + \hat{N}_{rsa}$ . The solution is described by

$$\begin{aligned} Q(\eta + \Delta\eta) &= \exp \left( \int_{\eta}^{\eta + \Delta\eta} (\hat{D}_{ds} + \hat{D}_{df} + \hat{N}_{nl}) d\eta' \right) Q(\eta) \\ &= \exp \left( (\hat{D}_{ds} + \hat{D}_{df}) \Delta\eta + \int_{\eta}^{\eta + \Delta\eta} \hat{N}_{nl} d\eta' \right) Q(\eta). \end{aligned} \quad (68)$$

Generally linear operators  $\hat{D}_{ds}$ ,  $\hat{D}_{df}$  and nonlinear operator  $\hat{N}_{nl}$  do not commute. In order to solve the propagation equation, we use the symmetric split-step method given by

$$Q(\eta + \Delta\eta) \approx e^{\frac{\Delta\eta}{2} \hat{D}_{df}} e^{\frac{\Delta\eta}{2} \hat{D}_{ds}} e^{\int_{\eta}^{\eta + \Delta\eta} \hat{N}_{nl} d\eta'} e^{\frac{\Delta\eta}{2} \hat{D}_{ds}} e^{\frac{\Delta\eta}{2} \hat{D}_{df}} Q(\eta). \quad (69)$$

Linear operators  $\hat{D}_{df}$  and  $\hat{D}_{ds}$  are solved in the frequency domain and the nonlinear operator  $\hat{N}_{nl}$  is solved in the time domain. The nonlinear operator  $\hat{N}_{nl}$  is solved using the trapezoid rule and then iterated until the solution converges

$$\int_{\eta}^{\eta + \Delta\eta} \hat{N}_{nl} [Q(\eta')] d\eta' \approx \frac{\Delta\eta}{2} \{ \hat{N}_{nl} [Q(\eta)] + \hat{N}_{nl} [Q(\eta + \Delta\eta)] \}. \quad (70)$$

In the first iteration  $\hat{N}_{nl} [Q(\eta + \Delta\eta)]$  is set equal to  $\hat{N}_{nl} [Q(\eta)]$  to obtain an initial value for  $Q(\eta + \Delta\eta)$  which is then used for  $\hat{N}_{nl} [Q(\eta + \Delta\eta)]$ . The process is repeated until convergence is achieved.

## 7 NUMERICAL CALCULATION

We consider a discrete time and space grid such as

$$\tau \rightarrow \tau_i, \quad \eta \rightarrow \eta_n, \quad \rho \rightarrow \rho_j. \quad (71)$$

For the fast Fourier transformation (FFT) algorithm, there must be exactly an integral power of 2 points equally spaced in the time domain

$$\tau_i = i\Delta\tau + \tau_{min}. \quad (72)$$

The  $\eta_n$  and  $\rho_j$  grids may be dynamically adjusted.

### 7.1 Diffraction Operator

The linear diffraction term in the frequency domain is given by

$$\frac{\partial \tilde{Q}}{\partial \eta} = \chi(\omega) \nabla_\rho^2 \tilde{Q}(\eta, \rho, \omega), \quad (73)$$

where  $\tilde{Q}(\eta, \rho, \omega)$  is the Fourier transform of  $Q(\eta, \rho, \tau)$ ,  $\chi(\omega) = i(1 - \sigma\omega)/4$  and  $\nabla_\rho^2$  is the radial Laplacian with azimuthal symmetry

$$\nabla_\rho^2 = \frac{1}{\rho} \frac{\partial}{\partial \rho} + \frac{\partial^2}{\partial \rho^2}. \quad (74)$$

This equation is solved using the following finite difference scheme.

$$\frac{\partial \tilde{Q}}{\partial \eta} = \frac{\tilde{Q}_{i,j}^{n+1} - \tilde{Q}_{i,j}^n}{\Delta \eta}, \quad (75)$$

and the Crank-Nicholson method

$$\nabla_\rho^2 \tilde{Q}(\eta_n, \rho, \omega) = \frac{1}{2} \left( \nabla_\rho^2 \tilde{Q}(\eta_n, \rho, \omega) + \nabla_\rho^2 \tilde{Q}(\eta_n + \Delta\eta, \rho, \omega) \right), \quad (76)$$

$$\nabla_\rho^2 \tilde{Q}(\eta_n, \rho, \omega) = \frac{1}{\rho_j} \frac{1}{4\Delta\rho} (\tilde{Q}_{i,j+1}^n - \tilde{Q}_{i,j-1}^n) + \frac{1}{2(\Delta\rho)^2} (\tilde{Q}_{i,j+1}^n - 2\tilde{Q}_{i,j}^n + \tilde{Q}_{i,j-1}^n), \quad (77)$$

where  $\Delta\rho = \rho_{j+1} - \rho_j$ . Then

$$\begin{aligned} \frac{\tilde{Q}_{i,j}^{n+1} - \tilde{Q}_{i,j}^n}{\Delta\eta} &= \frac{\chi(\omega_i)}{4\rho_j \Delta\rho} [\tilde{Q}_{i,j+1}^{n+1} - \tilde{Q}_{i,j-1}^{n+1} + \tilde{Q}_{i,j+1}^n - \tilde{Q}_{i,j-1}^n] \\ &\quad + \frac{\chi(\omega_i)}{2(\Delta\rho)^2} [\tilde{Q}_{i,j+1}^{n+1} - 2\tilde{Q}_{i,j}^{n+1} + \tilde{Q}_{i,j-1}^{n+1} + \tilde{Q}_{i,j+1}^n - 2\tilde{Q}_{i,j}^n + \tilde{Q}_{i,j-1}^n]. \end{aligned} \quad (78)$$

This equation can be rewritten as

$$U_{j,j-1}^i Q_{i,j-1}^{n+1} + U_{j,j}^i Q_{i,j}^{n+1} + U_{j,j+1}^i Q_{i,j+1}^{n+1} = V_{j,j-1}^i Q_{i,j-1}^n + V_{j,j}^i Q_{i,j}^n + V_{j,j+1}^i Q_{i,j+1}^n, \quad (79)$$

where

$$U_{j,j-1}^i = \frac{\chi(\omega_i) \Delta \eta}{2\Delta\rho} \left( \frac{1}{2\rho_j} - \frac{1}{\Delta\rho} \right), \quad (80)$$

$$U_{j,j}^i = 1 + \frac{\chi(\omega_i) \Delta \eta}{(\Delta\rho)^2}, \quad (81)$$

$$U_{j,j+1}^i = -\frac{\chi(\omega_i) \Delta \eta}{2\Delta\rho} \left( \frac{1}{2\rho_j} - \frac{1}{\Delta\rho} \right), \quad (82)$$

$$V_{j,j-1}^i = \frac{\chi(\omega_i) \Delta \eta}{2\Delta\rho} \left( \frac{1}{2\rho_j} - \frac{1}{\Delta\rho} \right), \quad (83)$$

$$V_{j,j}^i = 1 - \frac{\chi(\omega_i) \Delta \eta}{(\Delta\rho)^2}, \quad (84)$$

$$V_{j,j+1}^i = \frac{\chi(\omega_i) \Delta \eta}{2\Delta\rho} \left( \frac{1}{2\rho_j} + \frac{1}{\Delta\rho} \right), \quad (85)$$

which is valid for the interior points  $0 < \rho_i < \rho_{max}$ . For on axis points ( $\rho = 0$ ), the following facts are used; (1) for cylindrically symmetric systems  $\partial Q / \partial \rho = 0$  at  $\rho = 0$ , and (2) the Maclaurin expansion for  $\partial Q / \partial \rho$  is used to define  $\nabla_\rho^2$  at  $\rho = 0$  such as

$$Q'(\rho) = Q'(0) + \rho Q''(0) + \frac{1}{2} \rho^2 Q'''(0) + \dots, \quad (86)$$

$$\lim_{\rho \rightarrow 0} \frac{1}{\rho} Q'(\rho) = Q''(0). \quad (87)$$

Therefore, at the origin ( $\rho = 0$ ), the cylindrical heat equation becomes

$$\frac{\partial \tilde{Q}}{\partial \eta} = 2\chi(\omega) \frac{\partial^2 \tilde{Q}}{\partial \rho^2}. \quad (88)$$

Using the finite difference scheme described previously leads to

$$\frac{\tilde{Q}_{i,j}^{n+1} - \tilde{Q}_{i,j}^n}{\Delta \eta} = \frac{2\chi(\omega_i)}{\rho_{j+1} - \rho_{j-1}} \left[ \frac{\tilde{Q}_{i,j+1}^{n+1} - \tilde{Q}_{i,j}^{n+1} + \tilde{Q}_{i,j+1}^n - \tilde{Q}_{i,j}^n}{\rho_{j+1} - \rho_j} + \frac{\tilde{Q}_{i,j-1}^{n+1} - \tilde{Q}_{i,j}^{n+1} + \tilde{Q}_{i,j-1}^n - \tilde{Q}_{i,j}^n}{\rho_{j+1} - \rho_j} \right]. \quad (89)$$

At  $\rho = 0$ , i.e.,  $j = 0$  we can imagine extending the boundary to the left by a distance  $\rho_{-1}$  which introduces the fictitious quantity  $\tilde{Q}_{i,-1}^n$ . This quantity can be eliminated using the fact that

$$\left. \frac{\partial \tilde{Q}}{\partial \rho} \right|_{\rho=0} = 0, \quad \frac{\tilde{Q}_{i,1}^n - \tilde{Q}_{i,-1}^n}{\rho_1 - \rho_{-1}} = 0, \quad \tilde{Q}_{i,1}^n = \tilde{Q}_{i,-1}^n. \quad (90)$$

Therefore, if we assume that  $\rho_1 = \rho_{-1}$  then the equation to be solved is

$$\frac{\tilde{Q}_{i,0}^{n+1} - \tilde{Q}_{i,0}^n}{\Delta\eta} = \frac{2\chi(\omega_i)}{\rho_1^2} [\tilde{Q}_{i,1}^{n+1} - \tilde{Q}_{i,0}^{n+1} + \tilde{Q}_{i,1}^n - \tilde{Q}_{i,0}^n]. \quad (91)$$

Collecting terms this gives

$$U_{0,0}^i \tilde{Q}_{i,0}^{n+1} + U_{0,1}^i \tilde{Q}_{i,1}^{n+1} = V_{0,0}^i \tilde{Q}_{i,0}^n + V_{0,1}^i \tilde{Q}_{i,1}^n, \quad (92)$$

where

$$U_{0,0}^i = 1 + \frac{2\chi(\omega_i)\Delta\eta}{\rho_1^2}, \quad (93)$$

$$U_{0,1}^i = -\frac{2\chi(\omega_i)\Delta\eta}{\rho_1^2}, \quad (94)$$

$$V_{0,0}^i = 1 - \frac{2\chi(\omega_i)\Delta\eta}{\rho_1^2}, \quad (95)$$

$$V_{0,1}^i = -\frac{2\chi(\omega_i)\Delta\eta}{\rho_1^2}. \quad (96)$$

For the maximum radial point ( $\rho = \rho_N$ ) the finite difference expression is derived using following procedures. To compensate for the extended boundary point  $\rho_{N+1}$  the following assumption are made. First,  $\rho_{N+1}$  is symmetrically placed around  $\rho_N$ , i.e.

$$\rho_{N+1} - \rho_N = \rho_N - \rho_{N-1}, \quad \rho_{N+1} = 2\rho_N - \rho_{N-1}. \quad (97)$$

Second, the value of the function  $\tilde{Q}_{i,N+1}^n$  is determined by linear interpolation through the points  $\rho_{N-1}$ ,  $\rho_N$  and  $\rho_{N+1}$ ,

$$\frac{\tilde{Q}_{i,N+1}^n - \tilde{Q}_{i,N}^n}{\rho_{N+1} - \rho_N} = \frac{\tilde{Q}_{i,N}^n - \tilde{Q}_{i,N-1}^n}{\rho_N - \rho_{N-1}}, \quad \tilde{Q}_{i,N+1}^n = 2\tilde{Q}_{i,N}^n - \tilde{Q}_{i,N-1}^n. \quad (98)$$

Then the difference equation simplifies to

$$U_{N,N-1}^i \tilde{Q}_{i,N-1}^{n+1} + U_{N,N}^i \tilde{Q}_{i,N}^{n+1} = V_{N,N-1}^i \tilde{Q}_{i,N-1}^n + V_{N,N}^i \tilde{Q}_{i,N}^n, \quad (99)$$

where

$$U_{N,N-1}^i = \frac{2\chi(\omega_i)\Delta\eta}{2\rho_N(\rho_N - \rho_{N-1})}, \quad (100)$$

$$U_{N,N}^i = 1 - \frac{2\chi(\omega_i)\Delta\eta}{2\rho_N(\rho_N - \rho_{N-1})}, \quad (101)$$

$$V_{N,N-1}^i = -\frac{2\chi(\omega_i)\Delta\eta}{2\rho_N(\rho_N - \rho_{N-1})}, \quad (102)$$

$$V_{N,N}^i = 1 + \frac{2\chi(\omega_i)\Delta\eta}{2\rho_N(\rho_N - \rho_{N-1})}. \quad (103)$$

Now using the three finite difference expressions for the boundary points and the interior points, we can rewrite the expressions as a tri-diagonal matrix equation.

$$\hat{U}^i \tilde{Q}_{i,j}^{n+1} = \hat{V}^i \tilde{Q}_{i,j}^n, \quad \tilde{Q}_{i,j}^{n+1} = (\hat{U}^i)^{-1} \hat{V}^i \tilde{Q}_{i,j}^n, \quad (104)$$

where matrices  $\hat{U}^i$  and  $\hat{V}^i$  are tri-diagonal matrices which are determined by Eqs. (80-85), Eqs. (93-96), and Eqs. (100-103).  $\tilde{Q}_{i,j}^n$  is a column vector whose elements are  $\{\dots, \tilde{Q}_{i,j-1}^n, \tilde{Q}_{i,j}^n, \tilde{Q}_{i,j+1}^n, \dots\}$ . Using a general matrix equation solver, we can easily solve the above equation.

## 7.2 Dispersion Operator

In the frequency domain, the dispersion operator is given by Eq. (50) and the differential equation for dispersion is given as

$$\frac{\partial \tilde{Q}}{\partial \eta} = \hat{D}_{ds}(\omega) \tilde{Q}. \quad (105)$$

The solution becomes

$$\tilde{Q}(\eta + \Delta\eta/2, \rho, \omega) = e^{(\frac{i\gamma}{2}\omega^2 + \frac{i\delta}{6}\omega^3 - \frac{\Gamma}{2})\frac{\Delta\eta}{2}} \tilde{Q}(\eta, \rho, \omega). \quad (106)$$

## 7.3 Nonlinear Operator

The nonlinear operator is solved in the time domain using the trapezoid rule and then iterated until the algorithm converges.

$$\int_{\eta}^{\eta+\Delta\eta} d\eta' \hat{N}[Q(\eta')] = \frac{\Delta\eta}{2} \{ \hat{N}[Q(\eta)] + \hat{N}[Q(\eta + \Delta\eta)] \}. \quad (107)$$

In the first iteration  $\hat{N}[Q(\eta + \Delta\eta)]$  is set equal to  $\hat{N}[Q(\eta)]$  to obtain an estimate for  $Q(\eta + \Delta\eta)$  and the process is repeated until it converges. We consider a discrete time and space grid,

$$Q(\eta, \rho, \tau) \rightarrow Q(\eta_n, \rho_j, \tau_i) = Q_{ij}^n. \quad (108)$$

For  $\hat{N}(\eta)$ , we write

$$\hat{N}(\eta_n) = ip|Q_{ij}^n|^2. \quad (109)$$

The nonlinear part is comprised of simply multiplying the field in the time domain by the exponential

$$e^{\int_{\eta}^{\eta+\Delta\eta} C(\eta, \tau) d\eta} C(\eta, \tau) = e^{\frac{\Delta\eta}{2} \hat{N}(\eta + \Delta\eta, \rho, \tau)} e^{\frac{\Delta\eta}{2} \hat{N}(\eta, \rho, \tau)} C(\eta, \rho, \tau) \quad (110)$$

## 7.4 Rate Equation

The rate equations are

$$\frac{\partial \vec{N}}{\partial \tau} = T_0 \left\{ \hat{G} + \alpha |A_0|^2 |Q|^2 \hat{H} \right\} \vec{N}. \quad (111)$$

To solve this equation, we consider the following grid in the  $\eta - \tau$  plane where  $\square$  is the position of  $Q(\eta_n, \tau_i)$  and  $\bigcirc$  is the position of  $\vec{N}(\eta_{n+\frac{1}{2}}, \tau_{i-\frac{1}{2}})$ . Before the pulse enters the RSA material, all carriers are in the ground state. Therefore the initial condition for the carrier density is

$$\vec{N}(\eta_{n+\frac{1}{2}}, \tau_{i-\frac{1}{2}}) = \begin{pmatrix} 1 \\ 0 \\ 0 \\ 0 \\ 0 \end{pmatrix}. \quad (112)$$

For the propagation from  $Q(\eta_n, \tau_i)$  to  $Q(\eta_n, \tau_{i+1})$ , we assume the average carrier density is  $\frac{1}{2}[\vec{N}(\eta_{n-\frac{1}{2}}, \tau_{i+\frac{1}{2}}) + \vec{N}(\eta_{n+\frac{1}{2}}, \tau_{i+\frac{1}{2}})]$ . For the carrier excitation from  $\vec{N}(\eta_{n+\frac{1}{2}}, \tau_{i-\frac{1}{2}})$  to  $\vec{N}(\eta_{n+\frac{1}{2}}, \tau_{i+\frac{1}{2}})$ , we assume the average field is  $\frac{1}{2}[Q(\eta_n, \tau_i) + Q(\eta_{n+1}, \tau_i)]$ . The values  $Q(\eta_{n+1}, \tau_i)$  and  $\vec{N}(\eta_{n+\frac{1}{2}}, \tau_{i+\frac{1}{2}})$  are not determined before calculation. For the first iteration,  $Q(\eta_{n+1}, \tau_i)$  is set equal to  $Q(\eta_n, \tau_i)$ . The rate equations and the pulse propagation equation are iterated until the solutions converge. From the rate equation, we can get

$$\begin{aligned} \vec{N}(\eta_{n+\frac{1}{2}}, \tau_{i+\frac{1}{2}}) &= \exp \left( T_0 \int_{\tau_{i-\frac{1}{2}}}^{\tau_{i+\frac{1}{2}}} \left\{ \hat{G} + \alpha |A_0|^2 |Q|^2 \hat{H} \right\} d\tau' \right) \vec{N}(\eta_{n+\frac{1}{2}}, \tau_{i-\frac{1}{2}}) \\ &= \exp \left( \hat{G} T_0 \Delta \tau + \hat{H} \alpha |A_0|^2 T_0 \int_{\tau_{i-\frac{1}{2}}}^{\tau_{i+\frac{1}{2}}} |Q|^2 d\tau' \right) \vec{N}(\eta_{n+\frac{1}{2}}, \tau_{i-\frac{1}{2}}) \\ &\approx \exp \left( \hat{G} T_0 \Delta \tau + \hat{H} \alpha |A_0|^2 T_0 \Delta \tau \frac{1}{2} \left\{ |Q(\eta_n, \tau_i)|^2 + |Q(\eta_{n+1}, \tau_i)|^2 \right\} \right) \vec{N}(\eta_{n+\frac{1}{2}}, \tau_{i-\frac{1}{2}}) \\ &\approx \sum_{k=0}^{\infty} \frac{1}{k!} (\hat{R})^k \vec{N}(\eta_{n+\frac{1}{2}}, \tau_{i-\frac{1}{2}}), \end{aligned} \quad (113)$$

where  $\hat{R} = \hat{G} T_0 \Delta \tau + \hat{H} \alpha |A_0|^2 T_0 \Delta \tau \frac{1}{2} \{ |Q(\eta_n, \tau_i)|^2 + |Q(\eta_{n+1}, \tau_i)|^2 \}$ . We should choose  $\Delta \tau$  such that

$$|\hat{R}| \ll 1. \quad (114)$$

In our calculation, we keep terms up to  $k = 2$ .

## 8 ITERATION

The rate equations and the wave equation are given by

$$\frac{\partial \vec{N}}{\partial \tau} = T_0 \left\{ \hat{G} + \alpha |A_0|^2 |Q|^2 \hat{H} \right\} \vec{N}, \quad (115)$$

$$\frac{\partial Q}{\partial \eta} = [\hat{D}_{ds} + \hat{D}_{df} + \hat{N} + \hat{N}_{rsa}] Q, \quad (116)$$

If we consider only the  $\hat{N}_{rsa}$  term in the wave equation, then

$$\frac{\partial Q}{\partial \tau} = \hat{N}_{rsa} Q = -\frac{L_{df} N_T}{2} \vec{\sigma} \cdot \vec{N} Q. \quad (117)$$

The solutions are

$$\vec{N}(\eta_{n+\frac{1}{2}}, \tau_{i+\frac{1}{2}}) \approx \exp \left( T_0 \Delta \tau \hat{G} + T_0 \Delta \tau L_{df} \frac{1}{2} \left\{ |Q(\eta_n, t_i)|^2 + |Q(\eta_{n+1}, t_i)|^2 \right\} \hat{H} \right) \cdot \vec{N}(\eta_{n+\frac{1}{2}}, \tau_{i-\frac{1}{2}}), \quad (118)$$

$$Q(\eta_{n+1}, t_i) \approx \exp \left( -\frac{\Delta \eta}{2} \vec{\sigma} \cdot \left\{ \vec{N}(\eta_{n+\frac{1}{2}}, \tau_{i-\frac{1}{2}}) + \vec{N}(\eta_{n+\frac{1}{2}}, \tau_{i+\frac{1}{2}}) \right\} \right) Q(\eta_n, t_i). \quad (119)$$

The k-th and (k+1)-th iterated solutions are

$$\vec{N}^{(k)}(\eta_{n+\frac{1}{2}}, \tau_{i+\frac{1}{2}}) \approx \exp \left( T_0 \Delta \tau \hat{G} + T_0 \Delta \tau L_{df} \frac{1}{2} \left\{ |Q(\eta_n, t_i)|^2 + |Q^{(k)}(\eta_{n+1}, t_i)|^2 \right\} \hat{H} \right) \cdot \vec{N}(\eta_{n+\frac{1}{2}}, \tau_{i-\frac{1}{2}}), \quad (120)$$

$$Q^{(k+1)}(\eta_{n+1}, t_i) \approx \exp \left( -\frac{\Delta \eta}{2} \vec{\sigma} \cdot \left\{ \vec{N}(\eta_{n+\frac{1}{2}}, \tau_{i-\frac{1}{2}}) + \vec{N}^{(k)}(\eta_{n+\frac{1}{2}}, \tau_{i+\frac{1}{2}}) \right\} \right) Q(\eta_n, t_i). \quad (121)$$

Now consider the following errors

$$\begin{aligned} \vec{N}(\eta_{n+\frac{1}{2}}, \tau_{i+\frac{1}{2}}) - \vec{N}^{(k)}(\eta_{n+\frac{1}{2}}, \tau_{i+\frac{1}{2}}) &\approx \\ T_0 \Delta \tau L_{df} \frac{1}{2} \left\{ |Q(\eta_{n+1}, t_i)|^2 - |Q^{(k)}(\eta_{n+1}, t_i)|^2 \right\} \cdot \vec{N}^{(k)}(\eta_{n+\frac{1}{2}}, \tau_{i-\frac{1}{2}}), \end{aligned} \quad (122)$$

$$\begin{aligned} |Q(\eta_{n+1}, t_i)|^2 - |Q^{(k+1)}(\eta_{n+1}, t_i)|^2 &\approx \\ -\Delta \eta \frac{\Delta \tau}{2} \vec{\sigma} \cdot \hat{H} \cdot \vec{N}(\eta_{n+\frac{1}{2}}, \tau_{i-\frac{1}{2}}) |Q(\eta_n, t_i)|^2 \left\{ |Q(\eta_{n+1}, t_i)|^2 - |Q^{(k)}(\eta_{n+1}, t_i)|^2 \right\}. \end{aligned} \quad (123)$$

Then

$$\frac{\Delta \tilde{Q}^{(k+1)}}{\Delta \tilde{Q}^{(k)}} \approx -\frac{\Delta \eta}{\Delta \tau} 2 \vec{\sigma} \cdot \hat{H} \cdot \vec{N}(\eta_{n+\frac{1}{2}}, \tau_{i-\frac{1}{2}}) |Q(\eta_n, t_i)|^2, \quad (124)$$

where  $\Delta \tilde{Q}^{(k+1)} = |Q(\eta_{n+1}, t_i)|^2 - |Q^{(k)}(\eta_{n+1}, t_i)|^2$ . If the right hand-side of Eq. (127) is smaller than 1, then the iteration improves the accuracy of the solution .

## 9 SOLITON SOLUTION

To check the accuracy of our numerical method, we used the nonlinear Schrödinger equation (NLS) which has analytic solutions. By comparing the numerical solution to the analytic solution we verify the accuracy of our numerical method. The NLS equation is easily derived from our nonlinear wave equation and given by

$$i\frac{\partial U}{\partial \eta} + \frac{1}{2}\frac{\partial^2 U}{\partial \tau^2} + |U|^2 U = 0. \quad (125)$$

For certain case, Eq. (128) solitons. The fundamental soliton is given as

$$U(\eta, \tau) = \text{sech}(\tau)\exp(i\eta/2) \quad (126)$$

The intensity is independent of propagation distance  $\eta$ . Figure 3 shows the analytic solution and the numerical solution of Eq. (128). In the numerical calculation, we used a time step of  $\delta\tau = 0.05$  and a propagation step of  $\delta\eta = 0.000314$  for a total propagation distance of 3.14. The numerical solution agrees with the analytic solution yielding an error less than 0.5% for  $-2 < \tau < 2$  as shown in Figure 4. The error can be reduced by choosing a smaller propagation step and/or a smaller time step. In this calculation, we found that our numerical methods describe the soliton propagation very accurately.

## 10 CONCLUSION

In this report we described a numerical method for short optical pulse propagation in nonlinear media with RSA materials. Numerical solutions for soliton propagation are in excellent agreement with analytical solutions. In our numerical method, higher order group velocity dispersion terms, higher order nonlinear terms and the Raman term are easily incorporated for ultra-short pulse propagation. Five-level model reverse saturable absorbers(RSA) show optical limiting effect for appropriate input power intensities. For high power input pulse, the output pulse power is decreased significantly. Using our numerical results, we can design effective optical limiters for a given range of pulse powers.

## ACKNOWLEDGEMENTS

This research was sponsored in part by the Air Force Office of Scientific Research grant F49620-98-1-0256 (Courant Institute), Air Force Office of Scientific Research Laboratory Task (Brooks AFB) and AFRL/HEDB at Brooks AFB.

## References

- [1] J. H. Marburger, "Self-focusing: Theory," *Prog. Quant. Electr.* **4**, 35 (1975).
- [2] L. W. Tutt, and T. F. Boggess, "A Review of Optical Limiting Mechanisms and Devices using Organics, Fullerenes, Semiconductors and Other Materials," *Prog. Quant. Electr.* **17**, pp. 299–338, 1993.
- [3] I. C. Khoo, M. V. Wood, P. H. Chen, and M. Y. Shih, "Nonlinear Optical Liquid Cored Fiber Array and Liquid Crystalline Film for Optical Limiting of Frequency Agile Picosecond Pulsed-CW Laser," *Nonlinear Opt.* **21**, pp. 85–98, 1999.
- [4] S. Bartkiewicz, A. Miniewicz, F. Kajzar, and M. Zagórska, "All-optical Switching of Light in Hybrid Liquid Crystal Structures," *Nonlinear Opt.* **21**, pp. 99–114, 1999.
- [5] J. W. Perry, K. Mansour, S. R. Marder, K. J. Perry, D. Alvarez, and I. Choong, "Enhanced Reverse Saturable Absorption and Optical Limiting in Heavy-atom-substituted Phthalocyanines," *Opt. Lett.* **19**, pp. 625–627, 1994.
- [6] J. W. Perry, "Organic and Metal-Containing Reverse Saturable Absorbers for Optical Limiters," in *Nonlinear Optics of Organic Molecules and Polymers*, H. S. Nalwa, and S. Miyata, ed., pp. 813–840, CRC Press, New York, 1997.
- [7] T. Xia, D. J. Hagan, A. A. Said, and E. W. Van Stryland, "Optimized of Optical Limiting Devices Based on Excited-state Absorption," *Appl. Opt.* **18**, pp. 4110–4122, 1997.
- [8] R. Signorini, S. Sartori, M. Meneghetti, R. Bozio, M. Maggini, G. Scorrano, M. Prato, G. Brusatin, and M. Guglielmi, "Hybrid Sol-gel Glasses Containing Fullerene Derivatives for Bottleneck Optical Limiting with Multilayer Structures," *Nonlinear Opt.* **21**, pp. 143–162, 1999.
- [9] B. Hönerlage, J. Schell, and R. Levy, "Optical Limiting in  $C_{60}$  Doped Solid Sol-gel Glasses," *Nonlinear Opt.* **21**, pp. 189–200, 1999.
- [10] K. Mansour, M. J. Soileau, and E. W. Van Stryland, "Nonlinear Optical Properties of Carbon-black Suspensions (ink)," *J. Opt. Soc. Am. B* **9**, pp. 1100–1109, 1992.
- [11] D. Riehl, and F. Fougeant, "Thermodynamic Modeling of Optical Limiting Mechanisms in Carbon-black Suspensions (CBS)," *Nonlinear Opt.* **21**, pp. 391–399, 1999.
- [12] D. Beljonne, T. Kogej, S. R. Marder, J. W. Perry, and J. L. Brédas, "Theoretical Design of Organic Chromophores with Large Two-photon Absorption Cross-sections," *Nonlinear Opt.* **21**, pp. 461–480, 1999.

- [13] P. Feneyrou, D. Block, M. Pierre, A. Ibanez, and P. L. Baldeck, "Nonlinear Transmission of Optically Thick Two-photon Absorptive Materials," *Nonlinear Opt.* **21**, pp. 279–286, 1999.
- [14] E. L. Dawes, and J. H. Marburger, "Computer Studies in Self-focusing," *Phys. Rev.* **179**, pp. 862–868, 1969.
- [15] G. Luther, J. V. Moloney, A. Newell, and E. Wright, "Self-focusing threshold in normally dispersive media," *Opt. Lett.* **19**, pp. 862–864, 1994.
- [16] X. D. Cao, G. P. Agrawal, and C. J. McKinstrie, "Self-focusing of chirped optical pulses in media with normal dispersion," *Phys. Rev. A* **49**, pp. 4085–4092, 1994.
- [17] M. J. Potasek, and A. E. Paul, "Investigation of nonlinear ocular media using femtosecond laser pulses," *Proc. Laser and Noncoherent Ocular Effects: Epidemiology, Prevention, and Treatment, SPIE* **2974**, pp. 66–74, 1997.
- [18] M. J. Potasek, "Spatiotemporal Effects in Nonlinear Dispersive and Diffractive Media using Ultrashort Optical Pulses," *Nonlinear Opt.* **21**, pp. 399–412, 1999.
- [19] S. Kim, D. McLaughlin, and M. Potasek, "Propagation of the Electromagnetic Field in Optical Limiting Reverse Saturable Absorbers," *Phys. Rev. A* **61**, pp. 025801-1–025801-4, 2000.
- [20] G. P. Agrawal, *Nonlinear Fiber Optics*, Academic Press, New York, NY, 1995.
- [21] M. Potasek, S. Kim, and D. McLaughlin, "All-optical Power Limiting," accepted to *J. Nonlinear Opt. Materials and Phenomena*.

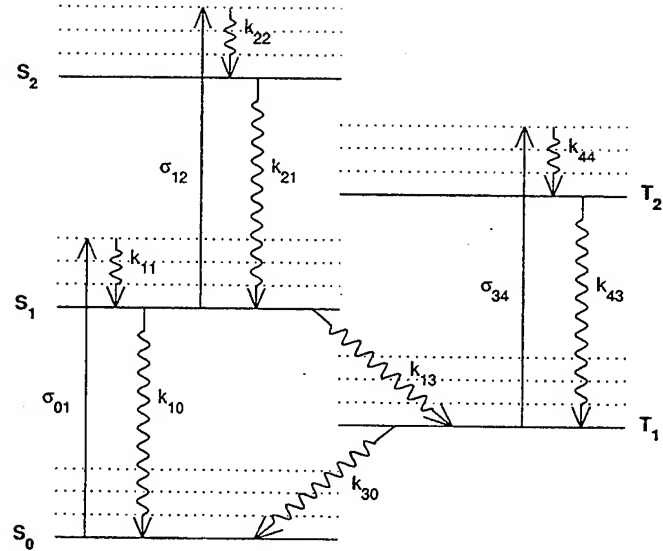


Figure 1: Schematic energy level for a chromophore. The electronic states are represented by solid horizontal lines and the vibronic states are represented by dotted horizontal lines.  $S_i$  represents a singlet state and  $T_i$  represents a triplet state. The photon absorption excitations are represented by solid vertical lines, and the decay processes are represented by wavy lines. The absorption coefficients  $\sigma_{ij}$  and the decay constants  $k_{ij}$  are described in the text. The physical values used for our calculations are:  $\sigma_{01} = 2.4 \times 10^{-18} \text{ cm}^2$ ,  $\sigma_{12} = 3.0 \times 10^{-17} \text{ cm}^2$ ,  $\sigma_{34} = 4.8 \times 10^{-17} \text{ cm}^2$ ,  $k_{10} = 0.144 \text{ ns}^{-1}$ ,  $k_{21} = 1.0 \text{ ps}^{-1}$ ,  $k_{13} = 77.8 \text{ ms}^{-1}$ ,  $k_{30} = 50.0 \text{ ms}^{-1}$ ,  $k_{43} = 1.0 \text{ ps}^{-1}$ , and  $k_{11}$ ,  $k_{22}$ ,  $k_{33}$  are due to vibrational decays which are assumed to be instantaneous.

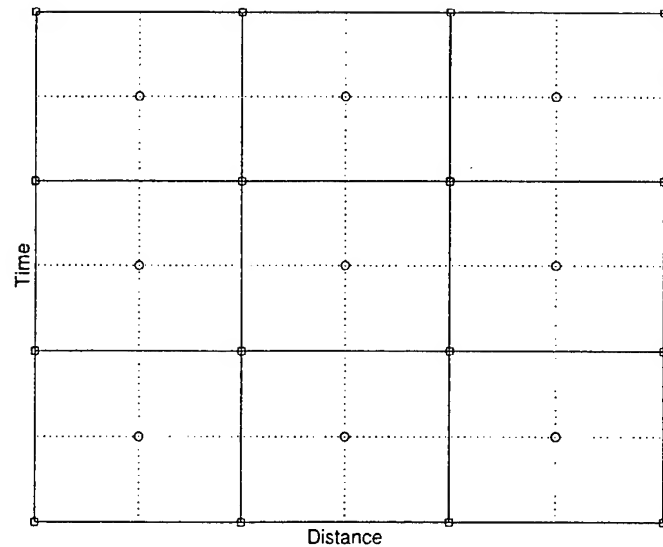


Figure 2: Space-Time grid for pulse propagation. Squares represent coordinates where pulse is calculated and circles represent coordinates where carrier densities are calculated.

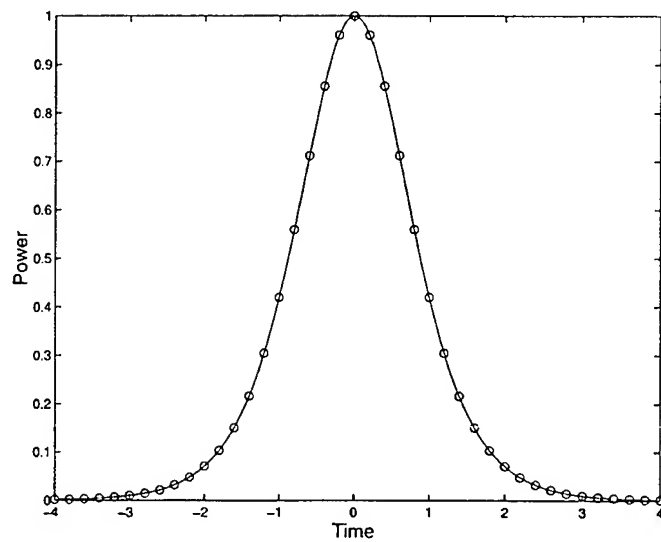


Figure 3: Analytic and numerical solution for the fundamental soliton propagation. The solid line shows the analytic solution and the circles show the numerical solution.

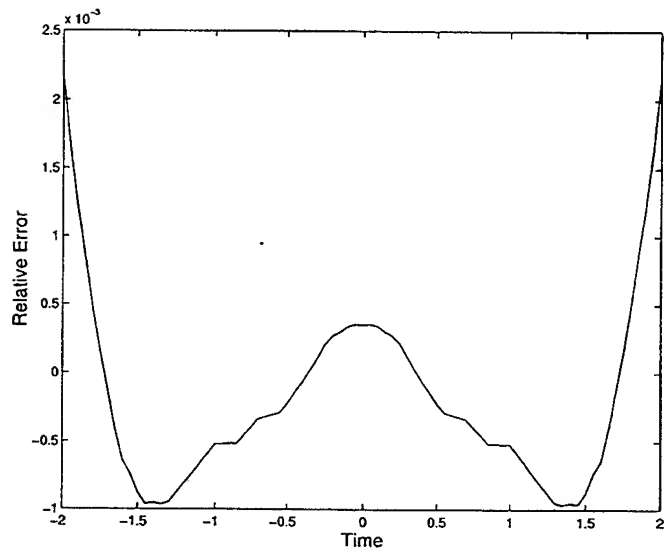


Figure 4: Relative error of and numerical solution for the fundamental soliton propagation.